

\mathcal{CP} -violation sensitivity of closed-shell radium-containing polyatomic molecular ionsKonstantin Gaul ^{1,*}, Nicholas R. Hutzler ², Phelan Yu ², Andrew M. Jayich,³ Miroslav Iliaš ⁴, and Anastasia Borschevsky⁵¹*Fachbereich Chemie, Philipps-Universität Marburg, Hans-Meerwein-Straße 4, 35032 Marburg, Germany*²*Division of Physics, Mathematics, and Astronomy, California Institute of Technology, Pasadena, California 91125, USA*³*Department of Physics, University of California, Santa Barbara, California 93106, USA*⁴*Department of Chemistry, Faculty of Natural Sciences, Matej Bel University, Tajovského 40, 97401 Banská Bystrica, Slovakia*⁵*Van Swinderen Institute for Particle Physics and Gravity, University of Groningen, 9747 AG Groningen, The Netherlands*

(Received 21 December 2023; accepted 1 March 2024; published 22 April 2024)

Closed-shell atoms and molecules such as Hg and TlF provide some of the best low-energy tests of hadronic \mathcal{CP} violation beyond the standard model of particle physics, which is considered to be a necessary ingredient to explain the observed excess of matter over antimatter in our universe. \mathcal{CP} violation is expected to be strongly enhanced in octupole-deformed nuclei such as ^{225}Ra . Recently, closed-shell radium-containing symmetric-top molecular ions were cooled sympathetically in a Coulomb crystal [Fan *et al.*, *Phys. Rev. Lett.* **126**, 023002 (2021)] and shown to be well suited for precision spectroscopy in the search for fundamental physics [Yu and Hutzler, *Phys. Rev. Lett.* **126**, 023003 (2021)]. In closed-shell molecules hadronic \mathcal{CP} violation contributes to a net electric dipole moment (EDM) that violates parity and time-reversal symmetries (\mathcal{P} , \mathcal{T}), which is the target of measurements. To interpret experiments, it is indispensable to know the electronic-structure-enhancement parameters for the various sources of \mathcal{P} , \mathcal{T} violation which contribute to the net \mathcal{P} , \mathcal{T} -odd EDM. We employ relativistic density-functional-theory calculations to determine relevant parameters for interpretation of possible EDM measurements in RaOCH_3^+ , RaSH^+ , RaCH_3^+ , RaCN^+ , and RaNC^+ and perform accurate relativistic coupled-cluster calculations of the Schiff-moment enhancement in RaSH^+ to gauge the quality of the density-functional-theory approach. Finally, we project to bounds on various \mathcal{P} , \mathcal{T} -odd parameters that could be achievable from an experiment with RaOCH_3^+ in the near future and assess its complementarity to experiments with Hg and TlF.

DOI: [10.1103/PhysRevA.109.042819](https://doi.org/10.1103/PhysRevA.109.042819)**I. INTRODUCTION**

Molecules and molecular ions provide some of the best probes of simultaneous violation of parity and time-reversal symmetries (\mathcal{P} , \mathcal{T} violation) [1]. Within the current experimental resolution a measurement of a \mathcal{P} , \mathcal{T} violation would be indirect evidence of a \mathcal{CP} violation beyond the standard model of particle physics [2], which is assumed to be necessary to explain the imbalance between matter and antimatter (baryon asymmetry) in our universe [3]. Recently, an experiment with the molecular ion HfF^+ tightened the upper bound on the electron electric dipole moment (eEDM) [4]. Whereas such experiments with open-shell molecules have been established for searching for \mathcal{P} , \mathcal{T} violation in the electron sector, experiments with closed-shell atoms such as mercury provide some of the best bounds on \mathcal{P} , \mathcal{T} violation in the hadronic sector [5]. Similar to polar open-shell molecules, \mathcal{P} , \mathcal{T} -odd effects in polar closed-shell molecules are enhanced by several orders of magnitude compared to the atom due to close-lying rotational states of opposite parity [6,7]. This will be exploited, for instance, in the upcoming Cold molecule Nuclear Time-Reversal EXperiment (CeNTREX) with TlF [8].

In addition to the benefits of relativistic enhancement of \mathcal{P} , \mathcal{T} violation in heavy atoms and molecules, the heaviest elements can possess isotopes with octupole deformation, which can significantly enhance the \mathcal{P} , \mathcal{T} -odd nuclear Schiff moment compared to spherical nuclei such as Tl or Hg [9,10]. In particular, ^{225}Ra was identified to possess a large octupole deformation [11,12] and is expected to have a strongly enhanced nuclear Schiff moment [13–16]. This nuclear enhancement is exploited in an experiment with ^{225}Ra [17,18], which is expected to be able to improve the bounds on \mathcal{CP} violation from the Hg experiment in the near future.

Recent developments make precision spectroscopy of molecules containing short-lived radioactive isotopes, such as ^{225}Ra , feasible [19–22]. Moreover, the proposal for direct laser cooling of polyatomic molecules [23] and its successive realization [24] were promptly followed by the exploration of the advantages of polyatomic molecules for EDM experiments [25–27]. Very close lying ℓ or K doublets can serve as internal comagnetometers and enable large polarization with weak electric fields, which renders symmetric-top and asymmetric-top molecules prospective candidates in the search for \mathcal{P} , \mathcal{T} violation [26].

Radium-containing polyatomic molecular ions combine these advantages of nuclear structure and molecular structure in a single system and can be expected to be exceptionally suitable for tightening bounds on hadronic \mathcal{CP} violation.

*konstantin.gaul@chemie.uni-marburg.de

Recently, efficient sympathetic cooling of trapped RaOH^+ and RaOCH_3^+ molecules with atomic radium ions in a Coulomb crystal was demonstrated [28]. In this context it was shown that RaOCH_3^+ has favorable properties for fundamental physics experiments, such as a large polarizability and opposite-parity states with tunable splittings [29]. Shortly afterward, the asymmetric-top molecular ion RaSH^+ was suggested as a promising candidate for precision experiments because it is assumed to have very close lying K doublets and was subsequently synthesized, trapped, and sympathetically cooled [30–32].

The extraction of bounds on \mathcal{CP} violation from experiments on a fundamental level requires electronic-structure-theory predictions of the molecular \mathcal{P} , \mathcal{T} -violation sensitivity coefficients. In this paper we provide these sensitivity coefficients for the symmetric-top molecules RaOCH_3^+ and RaCH_3^+ and the asymmetric-top molecule RaSH^+ and, for comparison, for the linear Ra-containing molecules RaNC^+ and RaCN^+ . Relativistic coupled-cluster theory is employed to estimate the influence of electron correlation on the molecular enhancement of the Schiff moment in RaSH^+ , which is achieved with an implementation of the Schiff-moment interaction operator into the DIRAC program package [33]. Enhancement of \mathcal{P} , \mathcal{T} violation in other molecules and from other possible fundamental sources is computed on the level of density-functional theory and subsequently used to estimate the sensitivity of an experiment with RaOCH_3^+ to relevant sources of \mathcal{P} , \mathcal{T} violation in comparison to experiments with Hg and TlF.

II. THEORY

A. Effective \mathcal{P} , \mathcal{T} -odd Hamiltonian

In a closed-shell asymmetric-top molecule such as RaSH^+ , which is polarized by an external electrical field of strength \mathcal{E} , the effective \mathcal{P} , \mathcal{T} -odd Hamiltonian is proportional to the interaction of the nuclear angular momentum \vec{I} with polarization axis $\vec{\lambda}$ in the molecular frame that can be defined by the principal axes of inertia \vec{a} , \vec{b} , and \vec{c} as

$$H_{\mathcal{P},\mathcal{T}} = \vec{I}^T \cdot \text{diag}(W_{\mathcal{P},\mathcal{T},a}, W_{\mathcal{P},\mathcal{T},b}, W_{\mathcal{P},\mathcal{T},c}) \cdot \vec{\lambda}, \quad (1)$$

where a , b , and c denote the components of the vectors in the principal-axis system. In a prolate symmetric-top molecule such as RaOCH_3^+ $b = c$. In analogy to hyperfine coupling constants, the b and c components contribute to an anisotropy of the \mathcal{P} , \mathcal{T} -odd interaction and vanish in a linear molecule. In closed-shell molecules the electronic-structure sensitivity

coefficients W are composed of individual contributions of sources of \mathcal{P} , \mathcal{T} violation as [34–36]

$$W_{\mathcal{P},\mathcal{T},a} = d_e W_{d,a}^m + d_{\text{sr},n} (\eta_A W_{m,a} + R_{\text{vol}} W_{S,a}) + \mathcal{S}_{\text{coll}} W_{S,a} + k_s W_{s,a}^m + k_T W_{T,a} + k_p W_{p,a}, \quad (2)$$

where d_e is eEDM, k_s is the scalar-pseudoscalar nucleon-electron current interaction constant, k_T is the tensor-pseudotensor nucleon-electron current interaction constant, and k_p is the pseudoscalar-scalar nucleon-electron current interaction constant. Closely following Ref. [37], the collective Schiff moment, which arises from the long-range nucleon-pion interactions, can be written as

$$\mathcal{S}_{\text{coll}} = g(a_0 \bar{g}_\pi^{(0)} + a_1 \bar{g}_\pi^{(1)} + a_2 \bar{g}_\pi^{(2)}), \quad (3)$$

where the strong pion-nucleon coupling strength is $g \approx 13.5$; $\bar{g}_\pi^{(0)}$, $\bar{g}_\pi^{(1)}$, and $\bar{g}_\pi^{(2)}$ are the nucleon-pion interaction constants; and a_0 , a_1 , and a_2 are the corresponding nuclear-structure-enhancement factors (see also Ref. [38]). $d_{\text{sr},n}$ is the remaining short-range contribution to the neutron EDM (nEDM), as defined, e.g., in Ref. [37] in a next-to-next-to-leading-order expansion of d_n , which contributes to the Schiff moment via the nuclear enhancement factor R_{vol} (see also [39]). References [40,41] showed that a single valence nucleon with an EDM will interact with the magnetic field produced by the electrons at the position of the nucleus with the nuclear-structure factor $\eta_A = \frac{\mu_N}{A_A} + \frac{\mu_A}{A_A - Z_A}$ with μ_N being the nuclear magneton, A_A , Z_A , and μ_A being the nuclear mass number, nuclear charge number, and nuclear magnetic moment of nucleus A , respectively. As the exact nuclear-structure relation between the nEDM and the hadronic sources of \mathcal{P} , \mathcal{T} violation is not known, we assume in the following the interaction with a single valence nucleon. Therefore, we neglect long-range nucleon-pion contributions to the nEDM, which would contribute to the magnetic interaction or via R_{vol} , as these contributions are at least three orders of magnitude smaller for heavy atoms and molecules than contributions from the collective Schiff moment (see Ref. [38] for details). These approximations do not impact the form of the electronic operators and allow us to obtain order-of-magnitude estimates of the sensitivity to sources of \mathcal{CP} violation at the hadronic level. However, to obtain rigorous bounds on fundamental sources of \mathcal{CP} violation a more sophisticated treatment of the nuclear structure would be required.

In the following we will drop the subscript a on all W when referring to the principal axis that points approximately along the Ra bonding axes. The individual electronic-structure factors W for the heavy Ra nucleus A are defined as (see Refs. [36,40,42–45])

$$\vec{W}_d^m = \frac{\mu_A}{I_A} \left[\left\langle \frac{2c\mu_0}{4\pi\hbar} \sum_{i=1}^{N_{\text{elec}}} \frac{i\gamma_i^0 \gamma_i^5 \hat{\ell}_{iA}}{r_{iA}^3} \right\rangle + 2\text{Re} \left\{ \sum_a \frac{\left\langle 0 \left| \frac{2c}{e\hbar} \sum_{i=1}^{N_{\text{elec}}} i\gamma_i^0 \gamma_i^5 \hat{D}_i^2 \right| a \right\rangle \left\langle a \left| \frac{\mu_0}{4\pi} \sum_{i=1}^{N_{\text{elec}}} \frac{\vec{r}_{iA} \times \vec{\alpha}_i}{r_{iA}^3} \right| 0 \right\rangle}{E_0 - E_a} \right\} \right], \quad (4)$$

$$\vec{W}_S = \left\langle -\frac{e}{\epsilon_0} \sum_{i=1}^{N_{\text{elec}}} (\vec{\nabla}_i \rho_A(\vec{r}_i)) \right\rangle, \quad (5)$$

$$\vec{W}_m = \left\langle 4 \frac{c\mu_0}{4\pi\hbar} \sum_{i=1}^{N_{\text{elec}}} \frac{\vec{\alpha}_i}{r_{iA}^3} \times \hat{\ell}_{iA} \right\rangle, \quad (6)$$

$$\vec{W}_s^m = \frac{\mu_A}{I_A} 2\text{Re} \left\{ \sum_a \frac{\left\langle 0 \left| \frac{-G_F Z_A}{\sqrt{2}} \sum_{i=1}^{N_{\text{elec}}} i \gamma_i^0 \gamma_i^5 \rho_A(\vec{r}_i) \right| a \right\rangle \left\langle a \left| \frac{\mu_0}{4\pi} \sum_{i=1}^{N_{\text{elec}}} \frac{\vec{r}_{iA} \times \vec{\alpha}_i}{r_{iA}^3} \right| 0 \right\rangle}{E_0 - E_a} \right\}, \quad (7)$$

$$\vec{W}_T = \left\langle \sqrt{2} G_F \sum_{i=1}^{N_{\text{elec}}} i \vec{\gamma} \rho_A(\vec{r}_i) \right\rangle, \quad (8)$$

$$\vec{W}_P = \left\langle -\frac{G_F \mu_N}{\sqrt{2} e c} \sum_{i=1}^{N_{\text{elec}}} \beta_i (\vec{\nabla}_i \rho_A(\vec{r}_i)) \right\rangle. \quad (9)$$

Here $\langle \cdot \rangle$ denotes the expectation value for a given many-electron wave function, and $|0\rangle$ and $|a\rangle$ denote wave functions of the electronic ground state and all excited states with energies E_0 and E_a , respectively. $i = \sqrt{-1}$ is the imaginary unit, c is the speed of light; \hbar is the reduced Planck constant; μ_0 is the magnetic constant; ϵ_0 is the electric constant; G_F is the Fermi constant, for which we employ the value $2.22249 \times 10^{-14} E_h a_0^3$; and μ_N is the nuclear magneton. \vec{r}_a , $\hat{p}_a = -i\hbar \vec{\nabla}_a$, and $\hat{\ell}_{ab} = -i\hbar \vec{r}_{ab} \times \vec{\nabla}_a$ are the position operator, momentum operator, and angular momentum operator of particle a relative to particle b , respectively. The relative position of two particles is $\vec{r}_{ab} = \vec{r}_a - \vec{r}_b$, and the distance operator is $r_{ab} = |\vec{r}_{ab}|$. ρ_A is the normalized nuclear-charge-density distribution of nucleus A . Z_A , I_A , and μ_A are the charge number, spin quantum number, and magnetic moment of nucleus A , respectively, which for ^{225}Ra are 88, 1/2, and $-0.7338\mu_N$ [46], respectively, and $\eta_A = \frac{\mu_N}{A_A} + \frac{\mu_A}{A_A - Z_A}$ is $-0.00091\mu_N$ for ^{225}Ra . We chose Dirac γ matrices defined as $\vec{\gamma} = \begin{pmatrix} 0 & \vec{\sigma} \\ -\vec{\sigma} & 0 \end{pmatrix}$, $\gamma^0 = \begin{pmatrix} 1 & 0 \\ 0 & -1 \end{pmatrix}$, $\beta = \gamma^0$, $\vec{\alpha} = \gamma^0 \vec{\gamma}$, and $\gamma^5 = i\gamma^0 \gamma^1 \gamma^2 \gamma^3$.

III. COMPUTATIONAL DETAILS

In this work we investigate the contributions from different sources of \mathcal{P} , \mathcal{T} violation to the level of Kohn-Sham (KS) density-functional theory (DFT) and Hartree-Fock (HF) calculations and benchmark our results on accurate relativistic coupled-cluster (CC) calculations of W_S . For this purpose we implemented the integrals of the derivative of the nuclear-charge-density distribution in the space of Gaussian basis functions χ_μ in the development version of the DIRAC program package [33] as

$$\langle \chi_\mu | \vec{\nabla} \rho_A | \chi_\nu \rangle = -2\zeta_A \langle \chi_\mu | \rho_A \vec{r}_A | \chi_\nu \rangle, \quad (10)$$

which are electric dipole moment integrals with a modified Gaussian density. These integrals are needed for the calculation of W_S and W_P . The current implementation was tested by comparison to the results obtained with the program developed in Ref. [35].

The Dirac matrix $i\vec{\gamma}$ was not available in the DIRAC program; only the time-reversal antisymmetric matrix $\vec{\gamma}$ was available. For calculations of W_T the DIRAC program thus had to be adjusted as described in the Appendix.

All relativistic four-component calculations, as well as calculations of properties in the Levy-Leblond approximation, the exact two-component approximation (X2C), and its

spin-free version (SFX2C), were performed with the development version of the program package DIRAC [33].

Dirac-KS (DKS) DFT calculations were performed within the local-density approximation (LDA) using the $X\alpha$ exchange functional [47,48] and the fifth correlation functional by Vosko, Wilk, and Nusair (VWN5) in Ref. [49]. In comparison to CC calculations DFT functionals tend to underestimate the \mathcal{P} , \mathcal{T} -odd effects, whereas HF usually overestimates them [35,36,50]. Therefore, we employed the hybrid LDA functional with 50% Fock exchange by Becke (BHandH) [51], which was found to give results that agree excellently with CC calculations [36]. Furthermore, we employed the Perdew-Burke-Ernzerhof (PBE) functional [52] and its hybrid version [53], as well as the Becke three-parameter Lee-Yang-Parr (B3LYP) hybrid exchange-correlation functional [54]. To benchmark the exchange-correlation functionals, we computed the enhancement of the Schiff moment in RaSH^+ on the level of Møller-Plesset perturbation theory of second order (MP2) and single-reference CC with single and double amplitudes (CCSD) and including perturbative triples [CCSD(T)]. At these correlated levels of theory, properties are computed in a finite-field approach by adding the perturbing operator with a small amplitude λ to the Hamiltonian:

$$\hat{H} = \hat{H}_0 + \lambda \hat{H}'. \quad (11)$$

The energy correction of first order in λ , $E^{(1)}$, is found by taking the numerical first derivative with respect to λ :

$$E^{(1)} = \left. \frac{\partial E}{\partial \lambda} \right|_{\lambda=0}. \quad (12)$$

In all these calculations we computed two points with $\lambda = \pm 1 \times 10^{-9}$ to take the numerical first derivative. The finite field is applied after the Dirac-HF (DHF) mean-field calculation is converged. Therefore, in this approach MP2 results are orbital unrelaxed (OU-MP2) and thus are expected to be strongly improved by the CCSD iterations.

Molecular-structure parameters of RaSH^+ and RaOCH_3^+ were optimized with the program package CFOUR [55,56] at the level of scalar relativistic SFX2C-CCSD(T) calculations employing an atomic-natural-orbital all-electron basis set of triple-zeta quality (ANO-RCC-TZVP) [57–59] up to a change in the geometry gradient of less than $10^{-5} E_{h/a_0}$ as a convergence criterion. Wave functions were optimized until the total energy change between two consecutive HF cycles was less than $10^{-10} E_h$ or better. The SFX2C-CCSD(T) method provides a good compromise between accuracy and

TABLE I. Bond lengths r and bond angles ϕ of various Ra-containing molecular ions with structure RaXY^+ optimized at the level of DKS-PBE0/dyall.cv3z (DKS) or, in the case of RaOCH_3^+ , at the level of SFX2C-CCSD(T)/ANO-RCC-TZVP [CCSD(T)]. In addition to DKS and CCSD(T), the structure parameters of RaSH^+ at the level of SFX2C-HF/dyall.cv3z (SFX2C-HF) and SFX2C-PBE0/dyall.cv3z (SFX2C-KS) are shown.

X	Y		$r(\text{Ra} - X)$ (Å)	$r(X - Y)$ (Å)	$\phi(\text{Ra} - X - Y)$ (deg)	$r(\text{C} - \text{H})$ (Å)	$\phi(X - \text{C} - \text{H})$ (deg)	$\phi(\text{H} - \text{C} - \text{H})$ (deg)
S	H	SFX2C-HF	2.87	1.33	98.2			
		CCSD(T)	2.81	1.34	89.9			
		SFX2C-KS	2.80	1.35	93.3			
		DKS	2.79	1.35	93.8			
O	CH ₃	CCSD(T)	2.19	1.41	180	1.09	111	108
		DKS	2.58			1.10	113	106
C	N	DKS	2.57	1.16	180			
N	C	DKS	2.40	1.18	180			

efficiency for the optimization of the molecular structure [60]. The molecular structure of RaSH^+ optimized in this way was compared to molecular-structure optimizations with the program package DIRAC at the level of SFX2C-HF, SFX2C-PBE0, and DKS-PBE0 with the Dyal's core-valence triple- ζ basis set (dyall.cv3z) basis set [61,62]. All other molecules were optimized at the level of DKS-PBE0/dyall.cv3z with DIRAC [61,62]. The optimized molecular-structure parameters are shown in Table I.

In all calculations with DIRAC, the nucleus was described as a normalized spherical Gaussian nuclear-charge-density distribution $\rho_A(\vec{r}) = \frac{\zeta_A^{3/2}}{\pi^{3/2}} e^{-\zeta_A|\vec{r}-\vec{r}_A|^2}$, with $\zeta_A = \frac{3}{2r_{\text{nuc},A}^2}$. The root-mean-square nuclear charge radius $r_{\text{nuc},A}$ was approximated depending on the nuclear mass number as suggested by Visscher and Dyal [63]. We used the isotopes ^1H , ^{12}C , ^{14}N , ^{16}O , ^{32}S and ^{226}Ra in all calculations. The influence of the exact nuclear mass number on properties is negligible for heavy atoms such as Ra.

IV. RESULTS

A. Assessment of uncertainty for the Schiff-moment enhancement in RaSH^+

In the following we estimate the errors of the calculated nuclear Schiff-moment-enhancement factors for the molecule RaSH^+ in detail by using sophisticated coupled-cluster approaches. This extensive study allows us to benchmark the DFT calculations, which we successively employ for other properties and molecules. For all calculations of RaSH^+ discussed in the following the molecular structure optimized at the level of SFX2C-CCSD(T)/ANO-RCC-TZVP was used if not stated otherwise.

1. Influence of the basis set on the mean-field level

The influence of the basis set was studied on the level of DHF for RaSH^+ comparing dyall.cv2z, dyall.cv3z, and dyall.cv4z [61,62]. From previous works [35,64] it is known that the Schiff-moment-enhancement operator is extremely sensitive to the wave function close to the nucleus, and one usually needs to add steep functions with exponents that are in the range of the exponent of the Gaussian nuclear-charge-density distribution. This region is weakly described in the used Dyal basis sets. Exponential factors ζ_i of the Gaussian

basis functions of the form $\exp(-\zeta_i r_i^2)$ of the steepest s and p functions are related by relatively large ratios ζ_i/ζ_j of the order of ~ 4 , and the Gaussians with the largest exponential factors are not steep enough to penetrate the nucleus. We added n steep s and m steep p functions with larger exponents, using the ratio of exponents ζ_i/ζ_j , where ζ_i and ζ_j are the largest and second-largest exponential factors in the basis set, to obtain the next-steepest s and p functions with exponent ζ_k as $\zeta_k = \zeta_i^2/\zeta_j$. This is indicated by “+nsmp” in the descriptor of the basis set. We also studied the influence of densifying the region of steep exponents by adding functions with exponential factors obtained as $\zeta_l = \zeta_i\sqrt{\zeta_i/\zeta_j}$ and for all additional ζ_k accordingly. This is indicated in the name of the basis by “(d)”. Finally, the influence of densifying the region of steep functions twice is studied by adding in addition functions with $\zeta_m = \zeta_i\sqrt[4]{\zeta_i/\zeta_j}$ [indicated by “(dd)”]. This study is summarized in Table II.

The double densification [cv3z + 2s2p(dd), cv4z + 2s2p(dd)] has no significant influence on the results, but we take this augmentation as a reference which describes the region in the nucleus best. All nonaugmented basis sets show large deviations from cv4z + 2s2p(dd). Even the dyall.cv4z basis results in an error of 5% for W_S . Adding a single steeper function in the s and p block reduces the error of the cv3z basis already by 7%. A densification of the steep functions finally converges the basis set on the DHF level. Adding only s functions is not enough to make the error smaller than 1%. In the following calculations we will use an augmentation with 2s2p and densification, i.e., in total five additional s and p functions [cv3z + 2s2p(d)].

2. Relativistic effects

To study the influence of relativistic effects we performed calculations in the nonrelativistic limit employing the Levy-Leblond Hamiltonian on the scalar relativistic (SFX2C) and two-component quasirelativistic levels employing the X2C scheme with and without the atomic mean-field two-electron spin-orbit coupling correction (AMFI) and on the full four-component Dirac-Coulomb (DC) and Dirac-Coulomb-Gaunt levels. We also computed the effect of explicitly considering the pure small-component two-electron integrals (SSSS). The results are summarized in Table III. We find that important relativistic effects are covered by more than 99% by using a

TABLE II. Influence of the basis set on the enhancement of the nuclear Schiff moment in RaSH⁺ on the level of DHF. In the last column the deviation relative to the dyall.cv4z basis set with additional 2s and 2p steep functions and double densification of the steep-function space [cv4z+2s2p(dd)] is shown.

Basis set	Steeper	Densified	$10^{-3} W_S$ (in units of $\frac{e}{4\pi\epsilon_0 a_0^3}$)	Deviation (%)
cv2z			-13.06	73.5
cv3z			-44.77	9.1
cv4z			-46.66	5.2
cv2z	1s1p	no	-45.69	7.2
cv3z	1s1p	no	-48.17	2.2
cv2z	2s2p	no	-46.10	6.4
cv3z	2s2p	no	-48.38	1.8
cv4z	2s2p	no	-48.31	1.9
cv3z	3s	yes	-47.32	3.9
cv2z	1s1p	yes	-49.01	0.5
cv3z	1s1p	yes	-49.23	0.0
cv2z	2s2p	yes	-48.83	0.8
cv3z	2s2p	yes	-49.22	0.0
cv4z	2s2p	yes	-49.29	0.0
cv3z	3s3p	yes	-49.22	0.0
cv3z	2s2p	double	-49.24	0.0
cv4z	2s2p	double	-49.24	

TABLE III. Influence of relativistic effects on the enhancement of the nuclear Schiff moment in RaSH⁺ at the level of DHF/cv3z+2s2p(d).

Method	$10^{-3} W_S$ (in units of $\frac{e}{4\pi\epsilon_0 a_0^3}$)	Increment (%)
Levy-Leblond	-4.734	
SFX2C	-69.84	+93.2
X2C	-48.83	+30.1
X2C+AMFI	-48.79	-0.1
DC	-49.22	+0.9
+Gaunt	-48.81	-0.8
+SSSS	-48.72	-0.2

TABLE IV. Influence of the active space on the RCCSD(T) electron-correlation effects in the enhancement of the nuclear Schiff moment in RaSH⁺. The first two columns show the lower and upper energy cutoffs for active spinors, respectively. In the third column the active space is given as *ninm*, where *n* is the number of electrons in *m* spinors. For the number of spinors a number in parentheses defines the number of spinors for the cv2z+2s2p(d) basis set, whereas a number without parentheses gives the number of spinors for the cv3z+2s2p(d) basis set. The number of digits corresponds to the numerical precision of the finite field CCSD(T) property gradient.

Lower cutoff (in units of E_h)	Upper cutoff (in units of E_h)	Active space	$10^{-3} W_S$ (in units of $\frac{e}{4\pi\epsilon_0 a_0^3}$)		
			cv2z+2s2p(d)	cv3z+2s2p(d)	cv3z
-2	10	16in300		-44.76	
-2	30	16in352		-44.70	
-2	100	16in420		-44.68	
-4	30	26in352(182)	-45.94	-45.06	-40.615
-4	100	26in420		-45.06	
-10	100	40in420		-44.71	
	10	104in(134)	-45.5		
	30	104in(182)	-45.5		
	100	104in(222)	-45.5		

two-component Hamiltonian, whereas considering only scalar relativistic effects overestimates the effect by about 30%. The influence of AMFI is negligible, and the corrections due to explicitly considering the full four-component Hamiltonian almost cancel with the Gaunt correction, which are both almost 1%. As we are doing coupled-cluster calculations in the following, the used Hamiltonian is not time critical, and we will employ the DC Hamiltonian for all following discussions. Currently, the Gaunt interaction cannot be included in the correlated calculations in DIRAC.

3. Electron-correlation effects

The size of the active space is studied on the level of CCSD(T) in Table IV. We were limited to using medium-size active spaces due to the enormous memory requirements. To circumvent this we studied the influence of larger active spaces with the cv2z + 2s2p(d) basis set.

We find that the active space does not have a large influence on the results on the level of CCSD(T). This is in contrast to our findings for the W_d parameters in BaF, BaOH, YbOH, and BaCH₃, where the core electrons have a significant effect on the calculated values [60,65,66]. Thus, we choose an active space of $[-4, 30] E_h$ as compromise that allows computations in a reasonable amount of time. The error of this approximation is estimated from our calculations to be on the order of 1%.

From a comparison of the very small cv2z + 2s2p(d) basis set with the cv3z + 2s2p(d) basis set for an active space of $[-4, 30] E_h$, we see that the influence of the basis set on the correlation effects on W_S is below 2%. The influence of the steep functions in the basis set is identical to the DHF level: The result with the cv3z basis set deviates by about 10% from the result with the cv3z + 2s2p(d) basis set.

The influence of including electron correlation up to a certain level was studied by comparing calculations at the levels of DHF, OU-MP2, CCSD, and CCSD(T) in Table V. Furthermore, we compare the results to different flavors of DFT. We find that the total correlation effect is only 9%. However, if we use DFT on the level of LDA or generalized gradient approximation, the effect of electron correlation is

TABLE V. Influence of electron correlation at the levels of OU-MP2, CCSD, CCSD(T), and DFT on the enhancement of the nuclear Schiff moment in RaSH⁺. All post-HF calculations are run with an active space of $[-4, 30] E_h$ and the cv3z+2s2p(d) basis set. Deviations (Dev.) from CCSD(T) calculations are shown in the third column.

Method	$10^{-3} W_S$ (in units of $\frac{e}{4\pi\epsilon_0 a_0^3}$)	Dev. (%)
DHF	-49.22	9.2
OU-MP2	-47.00	6.5
CCSD	-45.68	1.4
CCSD(T)	-45.06	
DKS-BHandH	-43.89	-2.6
DKS-PBE0	-41.44	-8.0
DKS-B3LYP	-40.52	-10.1
DKS-PBE	-37.00	-15.7
DKS-LDA	-37.16	-17.5

strongly overestimated, leading to too small values and deviations of more than 15%. Including 50% Fock exchange on the level of LDA (BHandH), the DFT error is reduced, and coupled-cluster results can be very well reproduced. This is in line with previous observations [35,36,50]. Thus, we will use the BHandH functional for the calculation of other properties.

The perturbative triples have only a small influence of 1.4% on the results. Based on this, we estimate the overall error due to the higher-order correlations to be below 2%.

4. Molecular-structure effects and vibrational corrections

We compare equilibrium molecular structures for RaSH⁺ optimized at different levels of theory in Table I. The influence of relativistic effects and electron-correlation effects on the structure was determined by a comparison of SFX2C-HF and SFX2C-CCSD(T) calculations as well as by comparing SFX2C-PBE0 and DKS-PBE0 calculations. The former comparison shows that correlation effects are important, in particular for the bonding angle between Ra, S, and H, which is overestimated by HF by about 8%. The comparison of the SFX2C-PBE0 and DKS-PBE0 calculations shows that spin-orbit coupling does not play a significant role for the structure of RaSH⁺. The influence of the molecular structure on the enhancement of the Schiff moment was determined at the level of DHF/cv3z + 2s2p(dd). With the molecular structure computed on the level of SFX2C-HF the value of the Schiff moment was found to be $-47.75 \times 10^3 \frac{e}{4\pi\epsilon_0 a_0^3}$, which deviates by about 3% from the result obtained using the SFX2C-CCSD(T) geometry ($-49.22 \times 10^3 \frac{e}{4\pi\epsilon_0 a_0^3}$). Thus, the slightly different HF structure has only a minor influence on the Schiff-moment enhancement. From this and the excellent agreement of molecular structures obtained at the PBE0 and CCSD(T) levels, we expect errors due to the equilibrium molecular structure on the Schiff-moment enhancement to be well below 1%. From considerations of vibrational corrections to enhancements of \mathcal{P} , \mathcal{T} violation in other polyatomic molecules such as YbOH [67,68] and RaOH [69] we can expect that vibrational corrections are well below 1% too. Therefore, we consider molecular-structure effects to be negligible at the present level of accuracy.

TABLE VI. Estimated uncertainties of the enhancement of the nuclear Schiff moment in RaSH⁺ predicted at the level of CCSD(T)/cv3z+2s2p(d) with active space $[-4, 30] E_h$.

Error source	Amount (%)
Molecular structure and vibrational corrections	< 1
Relativity	1
Basis set	2
Higher-order correlation	2
Active space	1
Total	< 7

5. Error budget

The overall error budget is summarized in Table VI, and we estimate the predicted value of W_S to be accurate within 7%. Our final value for the Schiff-moment enhancement in RaSH⁺ is $-45(3) \times 10^3 \frac{e}{4\pi\epsilon_0 a_0^3}$, which is favorably large and comparable to the enhancement in TIF ($W_S \sim 40 \times 10^3 \frac{e}{4\pi\epsilon_0 a_0^3}$ [64]), although not as large as, for instance, in multiply charged molecules such as PaF³⁺ and UF³⁺ [70,71].

B. \mathcal{P} , \mathcal{T} -odd electronic-structure-enhancement factors and projected limits

At the level of DKS-BHandH, we computed properties that are considered to be relevant for \mathcal{P} , \mathcal{T} violation in closed-shell molecules [see Eq. (2)] for RaSH⁺, RaOCH₃⁺, RaCH₃⁺, RaNC⁺, and RaCN⁺. The results are shown in Table VII. We find very similar enhancement effects for all compounds, and the influence of the substituents is small.

1. Anisotropy and asymmetry of \mathcal{P} , \mathcal{T} -odd coupling tensors in asymmetric-top molecules

As outlined in Sec. II, in an asymmetric-top molecule the electronic enhancement factors are rank-1 tensors in principle. As the moment of inertia along the Ra-S bond in RaSH⁺ is very small, coupling tensors will be similar to those of a linear molecule. Thus, no considerable enhancement effects along the principal axes perpendicular to the Ra-S bond can be expected. However, it is interesting to consider whether the asymmetry is different for different \mathcal{P} , \mathcal{T} -odd properties. This could be utilized in other systems with a larger difference in the principal axes to disentangle different contributions by measurements with different polarization directions. Although achieving controlled polarization in only one direction is already difficult for a polyatomic molecule, the different principal axes have been manipulated and studied with alternating fields for chiral spectroscopy [72], and such techniques could potentially be combined with measurement schemes which use alternating fields for \mathcal{P} , \mathcal{T} -violation searches [73–75].

In analogy to a diagonal rank-2 tensor we can define the isotropy $W_{\mathcal{P},\mathcal{A},\text{iso}}$, the anisotropy $W_{\mathcal{P},\mathcal{A},\text{ani}}$, and the asymmetry $W_{\mathcal{P},\mathcal{A},\text{asy}}$ as

$$W_{\mathcal{P},\mathcal{A},\text{iso}} = \frac{W_{\mathcal{P},\mathcal{A},a} + W_{\mathcal{P},\mathcal{A},b} + W_{\mathcal{P},\mathcal{A},c}}{3}, \quad (13)$$

TABLE VII. Electronic-structure-enhancement factors of \mathcal{P} , \mathcal{T} violation in Ra-containing closed-shell molecular ions computed at the level of DCKS-BHandH/dyall.cv3z+sp(d).

Molecule	W_d^m ($\frac{10^{20} \text{ Hz h}}{e \text{ cm}}$)	W_s^m (h Hz)	W_T (h kHz)	W_p (h Hz)	$W_m \eta_A$ ($\frac{10^{17} \text{ Hz h}}{e \text{ cm}}$)	W_S ($\frac{\text{MHz h}}{e \text{ fm}^3}$)
RaSH ⁺	31.9	82.9	-3.91	-15.3	-1.68	-1.95
RaOCH ₃ ⁺	34.9	93.4	-4.45	-17.5	-1.88	-2.23
RaCH ₃ ⁺	38.0	98.5	-4.62	-18.1	-1.91	-2.24
RaCN ⁺	32.5	86.4	-4.10	-16.1	-1.82	-2.06
RaNC ⁺	32.0	86.1	-4.10	-16.1	-1.82	-2.08

$$W_{\mathcal{P},\mathcal{T},\text{ani}} = \frac{2W_{\mathcal{P},\mathcal{T},a} - W_{\mathcal{P},\mathcal{T},b} - W_{\mathcal{P},\mathcal{T},c}}{3}, \quad (14)$$

$$W_{\mathcal{P},\mathcal{T},\text{asy}} = (W_{\mathcal{P},\mathcal{T},b} - W_{\mathcal{P},\mathcal{T},c})/W_{\mathcal{P},\mathcal{T},\text{ani}}. \quad (15)$$

For RaSH⁺ the isotropy and anisotropy are, in good approximation, proportional to $W_{\mathcal{P},\mathcal{T},a}$, as $W_{\mathcal{P},\mathcal{T},a}$ is expected to be much larger than the other two components. Thus, we focus on the asymmetry. We computed the b and c components of W_S and W_d for RaSH⁺ on the level of DKS-BHandH. The c components are zero within the numerical precision, and for the b components we find $W_{S,b} = 2 \frac{\text{kHz h}}{e \text{ fm}^3}$ and $W_{d,b} = 0.1 \frac{10^{20} \text{ Hz h}}{e \text{ cm}}$. As expected, the resulting asymmetry is negligibly small ($W_{S,\text{asy}} \sim -2 \times 10^{-3}$, $W_{d,\text{asy}} \sim 6 \times 10^{-3}$). Interestingly, the asymmetry for the eEDM enhancement differs considerably from the Schiff-moment-enhancement asymmetry, which reflects different ratios of W_S/W_d for different polarization directions. This could be valuable for the disentanglement of the different sources of \mathcal{P} , \mathcal{T} violation [36,37,76–78] in an experiment with an asymmetric-top molecule if polarization in different directions could be controlled. For RaSH⁺, effects are on the order of 10^{-3} and therefore too small to be relevant. It would be interesting to exploit larger differences between the principal components of \mathcal{P} , \mathcal{T} -odd enhancement factors, which can be expected in heavy-element-containing chiral molecules, in which other parity-violating forces beyond the standard model of particle physics are favorably enhanced [79,80].

2. Projected limits on sources of \mathcal{P} , \mathcal{T} violation

Reference [29] gave the estimated experimental sensitivity for precession frequency measurements on a single trapped

²²⁵RaOCH₃⁺ ion with 2 weeks of data, taken to be $\delta\nu = (7.5 \text{ mrad/s})/(\sqrt{336}/2\pi) = 6.5 \times 10^{-5} \text{ Hz}$. Assuming this sensitivity, we can project limits on sources of \mathcal{P} , \mathcal{T} violation from an experiment with ²²⁵RaOCH₃⁺ within single-source models, i.e., assuming only a single source of \mathcal{P} , \mathcal{T} violation exists at a time.

For the collective Schiff moment of ²²⁵Ra we use recommended values from Ref. [38]:

$$a_0 = -1.5 e \text{ fm}^3, \quad a_1 = 6 e \text{ fm}^3, \quad a_2 = -4 e \text{ fm}^3. \quad (16)$$

To our best knowledge there is no calculation for R_{vol} available. In order to obtain a rough order-of-magnitude estimate of the sensitivity of an experiment with ²²⁵RaOCH₃⁺ in comparison to the TIF and Hg experiments we use the crude rule-of-thumb approximation discussed in Ref. [39]: $R_{\text{vol}} \sim \frac{1}{10} (1.2 \text{ fm})^{\frac{2}{3}} A^{2/3} = \frac{1}{10} (1.2 \text{ fm})^{\frac{2}{3}} \times 225^{2/3} = 3.2 \text{ fm}^2$. To obtain rigorous bounds on the underlying sources of \mathcal{P} , \mathcal{T} violation a more sophisticated treatment of the nuclear structure will be required.

In Table VIII we compare the resulting projected sensitivities for RaOCH₃⁺ with the single-source limits of the Hg [5] and TIF [81] experiments, which we computed from the electronic-structure data provided in Ref. [36] and nuclear-structure data summarized in Ref. [38]. We want to note that RaOCH₃⁺ and Hg are sensitive to the nEDM, whereas TIF is sensitive to the proton EDM, which we give here within our rough approximation as the short-range contribution to the proton EDM $d_{\text{sr,p}}$. Moreover, open-shell molecules such as HfF⁺, ThO, and RaF are generally much more sensitive to d_e and k_s , which we will, therefore, not discuss in the following.

We find that an experiment with even a single RaOCH₃⁺ molecule will have sensitivity to \mathcal{P} , \mathcal{T} violation comparable

TABLE VIII. Projected single-source limits on parameters of \mathcal{P} , \mathcal{T} violation from a proposed experiment with a single RaOCH₃⁺ molecular ion compared to the Hg [5] and TIF [81] experiments. Limits are derived from the projected experimental sensitivity of an experiment with RaOCH₃⁺ $\delta\nu \approx 6.5 \times 10^{-5} \text{ Hz}$ [29], the electronic-structure-enhancement factors given in Table VII, and the nuclear-structure factors discussed in the text.

System	d_e (e cm)	$d_{\text{sr,n}}$ (e cm)	$d_{\text{sr,p}}$ (e cm)	k_s	k_T	k_p	$g_\pi^{(0)}$	$g_\pi^{(1)}$	$g_\pi^{(2)}$
TIF ^a	6×10^{-26}		2×10^{-22}	2×10^{-6}	6×10^{-8}	2×10^{-5}	8×10^{-10}	7×10^{-11}	4×10^{-10}
Hg ^a	3×10^{-27}	3×10^{-26}		2×10^{-8}	2×10^{-10}	4×10^{-8}	2×10^{-12}	1×10^{-12}	1×10^{-12}
RaOCH ₃ ⁺	4×10^{-26}	2×10^{-24}		2×10^{-6}	3×10^{-8}	8×10^{-6}	3×10^{-12}	8×10^{-13}	2×10^{-12}

^aValues are computed with the experimental uncertainty of the EDM of TIF $\sigma_d = 2.9 \times 10^{-23} e \text{ cm}$ with an external electric field for polarization of strength $\mathcal{E} = 16000 \text{ V cm}^{-1}$ from Ref. [81] and the EDM of Hg $\sigma_d = 3.1 \times 10^{-30} e \text{ cm}$ from Ref. [5]. Electronic-structure-enhancement factors W for Hg and TIF were computed at the level of DFT within zeroth order regular approximation using the BHandH functional in Ref. [36]. Nuclear-structure factors are taken from Ref. [38].

to that of the Hg experiment for certain underlying sources. In particular, the single-molecule experiment with RaOCH_3^+ would place similar bounds on pion-nucleon couplings $\bar{g}_\pi^{(0)}$, $\bar{g}_\pi^{(1)}$, and $\bar{g}_\pi^{(2)}$ and therefore similar bounds on the \mathcal{CP} -violation parameter $\bar{\theta} \sim \bar{g}_\pi^{(0)}/0.015$ [82] and quark EDMs $\bar{d}_d - \bar{d}_u \sim 5 \times 10^{-15} \text{ e cm } \bar{g}_\pi^{(1)}$ [38]. In comparison to the TIF experiment of Ref. [81], only a slightly increased sensitivity can be expected for the electron-nucleon current interactions, whereas sensitivity to pion-nucleon couplings is increased by at least 2 orders of magnitude. The sensitivity of the TIF experiment is expected to be improved by roughly 3 orders of magnitude in the upcoming CeNTREX experiment with TIF, for which a frequency shift of $\delta\nu = 50 \times 10^{-9} \text{ Hz}$ is claimed to be achievable [8]. Taking this projected sensitivity for TIF would surpass all single-source bounds from Hg and an experiment with a single RaOCH_3^+ . Having a valence proton and therefore sensitivity to $d_{\text{sr,p}}$ instead of $d_{\text{sr,n}}$, TIF would, at any rate, be complementary to RaOCH_3^+ .

The limits here are given for a single trapped RaOCH_3^+ molecule with a coherence time of $\tau = 5 \text{ s}$ limited by blackbody pumping at 300 K [29]. Increasing the coherence time by a factor of t , which would require using a cryogenic apparatus, and trapping $N > 1$ ions at a time [4,83,84] would increase the sensitivity by a factor of \sqrt{tN} , as would using quantum-enhanced metrology to beat the standard quantum limit [75]. Experimental efforts to realize these advances are currently underway.

The single-source assumption is not a realistic model [36,37,76], and in a global model for \mathcal{P} , \mathcal{T} violation the polyatomic Ra-containing molecular ions will be very beneficial because ratios between different sensitivity coefficients vary considerably compared to Hg and TIF. The complementarity of RaOCH_3^+ to Hg and TIF is illustrated for the two-dimensional subspaces of the considered \mathcal{P} , \mathcal{T} -odd parameter space in Fig. 1, as suggested in Ref. [36]. The subspaces which include the parameters d_e , $d_{\text{sr,p}}$, and k_s , to which the RaOCH_3^+ molecule is rather insensitive compared to open-shell systems and systems with a valence proton, are shown in the Supplemental Material [85]. Figure 1 highlights the complementary sensitivity to pion-nucleon interactions of Ra-containing polyatomic ions compared to the Hg experiment.

V. CONCLUSION

We have computed electronic-structure enhancement of \mathcal{P} , \mathcal{T} violation in radium containing molecular ions with closed electronic shells, which are promising candidates for precision tests of fundamental symmetry violation in the hadronic sector. We implemented the Schiff-moment interaction operator in DIRAC for performing accurate coupled-cluster calculations to gauge the importance of electron correlation for this effect in the asymmetric-top molecule RaSH^+ . The suggested value for the Schiff-moment enhancement in RaSH^+ is $-45(3) \times 10^3 \frac{e}{4\pi\epsilon_0 a_0^4}$. Subsequently, we used this approach to benchmark DFT functionals for the computation of enhancement factors for various possible sources of \mathcal{P} , \mathcal{T} violation in several polyatomic radium-containing molecular ions. The asymmetry of \mathcal{P} , \mathcal{T} -violation enhancement in RaSH^+ was studied using DFT. Although this effect is too small to be relevant in

RaSH^+ , our findings indicate that asymmetric-top molecules which deviate strongly from prolate or oblate rotors may provide an interesting route for disentanglement of sources of \mathcal{P} , \mathcal{T} violation via measurements with different polarization directions. Finally, we computed projected \mathcal{P} , \mathcal{T} -violation sensitivities of an experiment with a single RaOCH_3^+ molecule. Our results show that enhancements in radium-containing polyatomic molecular ions are favorably large and are complementary to those in the TIF and Hg experiments.

ACKNOWLEDGMENTS

K.G. is indebted to R. Berger for support and acknowledges the Deutsche Forschungsgemeinschaft (DFG, German Research Foundation), Project No. 328961117, SFB 1319 ELCH, and the Haeuser-Stiftung for funding a research stay in Groningen. K.G. thanks P. A. B. Haase, Y. M. Comorro Mena, and I. A. Aucar for discussions. A.M.J. acknowledges support from the U.S. Department of Energy (Grant No. DE-SC0022034). N.R.H. acknowledges support from NSF CAREER Award No. PHY-1847550. Computer time on the Peregrine high-performance computing cluster provided by the Center for Information Technology of the University of Groningen is gratefully acknowledged.

APPENDIX: IMPLEMENTATION OF W_T

Each matrix in the vector $i\beta\vec{\alpha}$ can be decomposed in a quaternion scalar and a *real-valued* matrix in the space of the large and small component spinors:

$$-i\beta\vec{\alpha} = -i\sigma_y \otimes i\vec{\sigma} \equiv \begin{pmatrix} \hat{k} \\ \hat{j} \\ \hat{i} \end{pmatrix} \otimes (-i\sigma_y) = \begin{pmatrix} \hat{k} \\ \hat{j} \\ \hat{i} \end{pmatrix} \otimes \begin{pmatrix} 0 & -1 \\ 1 & 0 \end{pmatrix}, \quad (\text{A1})$$

where \hat{i} , \hat{j} , and \hat{k} are the quaternion units that correspond to the space spanned by $i\vec{\sigma}$, with $i = \sqrt{-1}$ being the imaginary unit. This matrix is time reversal symmetric and can be combined with antisymmetric real-valued basis-function integrals to form Hermitian operators. In the DIRAC program the matrix defined under the name **iBETAAL** ($i\beta\vec{\alpha}$) is of the form

$$\begin{pmatrix} \hat{j} \\ \hat{k} \\ 1 \end{pmatrix} \otimes \begin{pmatrix} 0 & -1 \\ 1 & 0 \end{pmatrix}. \quad (\text{A2})$$

For the computation of W_T the definition of **iBETAAL** in DIRAC was modified to

$$\begin{pmatrix} \hat{k} \\ \hat{j} \\ \hat{i} \end{pmatrix} \otimes \begin{pmatrix} 0 & -1 \\ 1 & 0 \end{pmatrix}. \quad (\text{A3})$$

The resulting time-reversal-symmetric density matrix is combined with the antisymmetric real-valued integrals of the normalized nuclear-charge-density-distribution operator ρ_A .

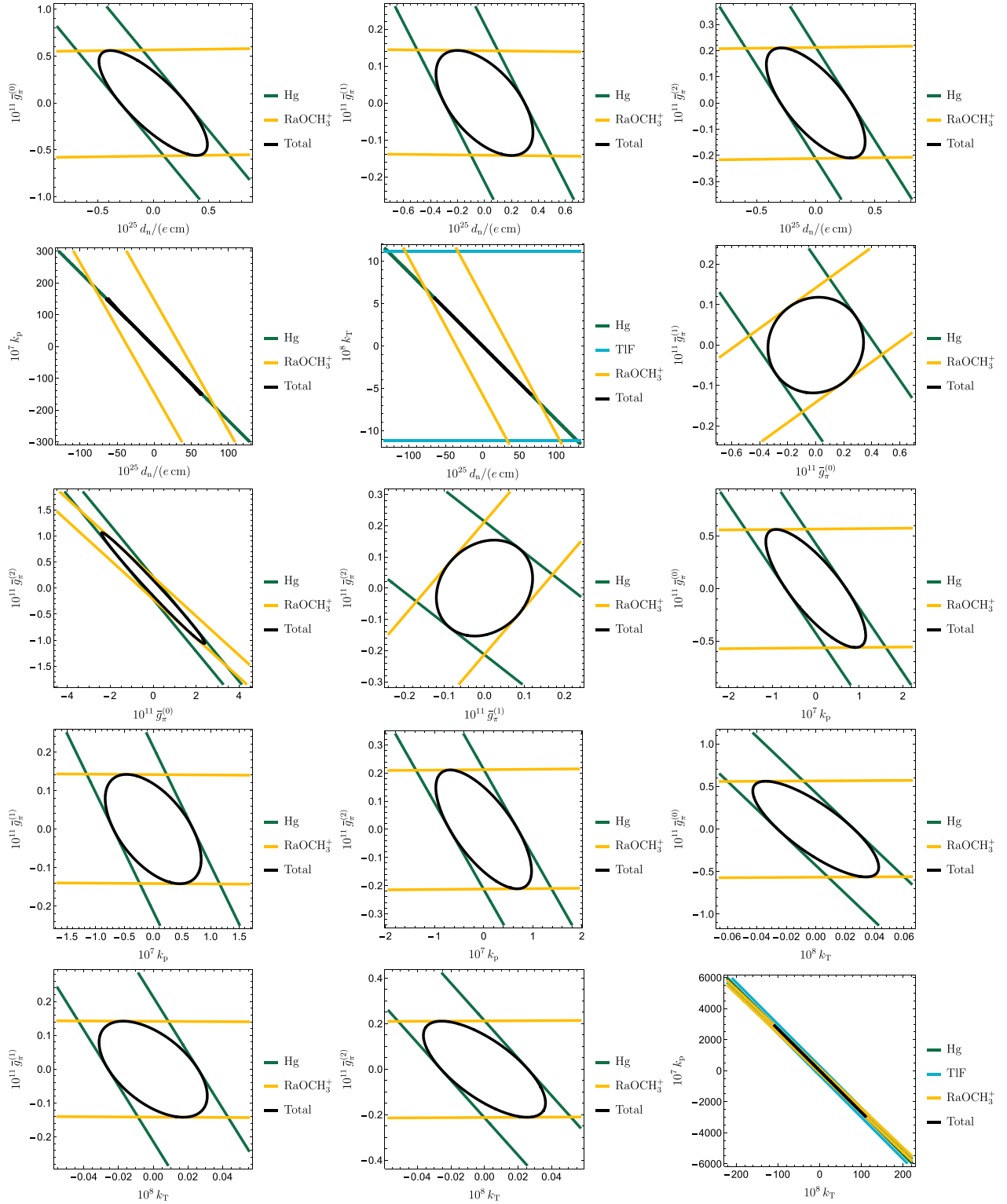


FIG. 1. Restriction of two-dimensional subspaces including parameters $d_{sr,n}$, k_T , k_p , $g_\pi^{(0)}$, $g_\pi^{(1)}$, and $g_\pi^{(2)}$ of the considered nine-dimensional space of P, T -odd parameters in experiments with Hg and TIF and the proposed experiment with RaOCH_3^+ . Coverage regions are computed with electronic-structure parameters of RaOCH_3^+ provided in this work, electronic-structure parameters of TIF and Hg from Ref. [36], and nuclear-structure parameters from Ref. [38]. The experimental uncertainty of the EDM of TIF $\sigma_d = 2.9 \times 10^{-23} e \text{ cm}$ with an external electric field for a polarization of strength $\mathcal{E} = 16000 \text{ Vcm}^{-1}$ is taken from Ref. [81], and that of the EDM of Hg $\sigma_d = 3.1 \times 10^{-30} e \text{ cm}$ is taken from Ref. [5]. The expected uncertainty of an experiment with a single RaOCH_3^+ molecule $\delta\nu \approx 6.5 \times 10^{-5} \text{ Hz}$ is used as proposed in Ref. [29]. All bounds are computed with Gaussian probability distributions of 95% confidence level as described in Ref. [36]. The two-dimensional subspaces that include the parameters d_e , $d_{sr,p}$, and k_s are shown in the Supplemental Material.

- [1] D. DeMille, *Phys. Today* **68**(12), 34 (2015).
- [2] I. B. Khriplovich and S. K. Lamoreaux, *CP Violation without Strangeness* (Springer, Berlin, 1997).
- [3] A. D. Sakharov, *JETP Lett.* **5**, 24 (1967).
- [4] T. S. Roussy, L. Caldwell, T. Wright, W. B. Cairncross, Y. Shagam, K. B. Ng, N. Schlossberger, S. Y. Park, A. Wang, J. Ye, and E. A. Cornell, *Science* **381**, 46 (2023).
- [5] B. Graner, Y. Chen, E. G. Lindahl, and B. R. Heckel, *Phys. Rev. Lett.* **116**, 161601 (2016).
- [6] L. N. Labzowsky, *Sov. Phys. JETP* **48**, 434 (1978).
- [7] V. G. Gorshkov, L. N. Labzovskii, and A. N. Moskalev, *Zh. Eksp. Teor. Fiz.* **76**, 414 (1979) [*Sov. Phys. JETP* **49**, 209 (1979)].
- [8] O. Grasdijk, O. Timgren, J. Kastelic, T. Wright, S. Lamoreaux, D. DeMille, K. Wenz, M. Aitken, T. Zelevinsky, T. Winick, and D. Kawall, *Quantum Sci. Technol.* **6**, 044007 (2021).
- [9] W. C. Haxton and E. M. Henley, *Phys. Rev. Lett.* **51**, 1937 (1983).
- [10] N. Auerbach, V. V. Flambaum, and V. Spevak, *Phys. Rev. Lett.* **76**, 4316 (1996).
- [11] P. A. Butler and W. Nazarewicz, *Rev. Mod. Phys.* **68**, 349 (1996).
- [12] P. A. Butler, *Proc. R. Soc. A.* **476**, 20200202 (2020).
- [13] V. Spevak, N. Auerbach, and V. V. Flambaum, *Phys. Rev. C* **56**, 1357 (1997).
- [14] J. Dobaczewski and J. Engel, *Phys. Rev. Lett.* **94**, 232502 (2005).
- [15] N. Yamanaka, B. K. Sahoo, N. Yoshinaga, T. Sato, K. Asahi, and B. P. Das, *Eur. Phys. J. A* **53**, 54 (2017).
- [16] J. Dobaczewski, J. Engel, M. Kortelainen, and P. Becker, *Phys. Rev. Lett.* **121**, 232501 (2018).
- [17] R. H. Parker, M. R. Dietrich, M. R. Kalita, N. D. Lemke, K. G. Bailey, M. Bishof, J. P. Greene, R. J. Holt, W. Korsch, Z.-T. Lu, P. Mueller, T. P. O'Connor, and J. T. Singh, *Phys. Rev. Lett.* **114**, 233002 (2015).
- [18] M. Bishof, R. H. Parker, K. G. Bailey, J. P. Greene, R. J. Holt, M. R. Kalita, W. Korsch, N. D. Lemke, Z.-T. Lu, P. Mueller, T. P. O'Connor, J. T. Singh, and M. R. Dietrich, *Phys. Rev. C* **94**, 025501 (2016).
- [19] R. F. Garcia Ruiz *et al.*, *Nature (London)* **581**, 396 (2020).
- [20] S. M. Udrescu *et al.*, *Phys. Rev. Lett.* **127**, 033001 (2021).
- [21] S. M. Udrescu *et al.*, *Nat. Phys.* **20**, 202 (2024).
- [22] S. G. Wilkins *et al.*, [arXiv:2311.04121](https://arxiv.org/abs/2311.04121).
- [23] T. A. Isaev and R. Berger, *Phys. Rev. Lett.* **116**, 063006 (2016).
- [24] I. Kozryyev, L. Baum, K. Matsuda, B. L. Augenbraun, L. Anderegg, A. P. Sedlack, and J. M. Doyle, *Phys. Rev. Lett.* **118**, 173201 (2017).
- [25] T. A. Isaev, A. V. Zaitsevskii, and E. Eliav, *J. Phys. B* **50**, 225101 (2017).
- [26] I. Kozryyev and N. R. Hutzler, *Phys. Rev. Lett.* **119**, 133002 (2017).
- [27] L. Anderegg, N. B. Vilas, C. Hallas, P. Robichaud, A. Jadbabaie, J. M. Doyle, and N. R. Hutzler, *Science* **382**, 665 (2023).
- [28] M. Fan, C. A. Holliman, X. Shi, H. Zhang, M. W. Straus, X. Li, S. W. Buechele, and A. M. Jayich, *Phys. Rev. Lett.* **126**, 023002 (2021).
- [29] P. Yu and N. R. Hutzler, *Phys. Rev. Lett.* **126**, 023003 (2021).
- [30] N. Hutzler and P. Yu, *Bull. Am. Phys. Soc.* **66**, K03.00009 (2021).
- [31] A. Jayich, New Opportunities for Fundamental Physics Research with Radioactive Molecules Virtual Meeting, June 28–July 2, 2021, <https://web.mit.edu/radiomolecules/program.html>.
- [32] G. Arrowsmith-Kron *et al.*, [arXiv:2302.02165](https://arxiv.org/abs/2302.02165).
- [33] DIRAC, a relativistic ab initio electronic structure program, Release DIRAC23 (2023), written by R. Bast, A. S. P. Gomes, T. Saue and L. Visscher and H. J. Aa. Jensen, with contributions from I. A. Aucar, V. Bakken, C. Chibueze, J. Creutzberg, K. G. Dyall, S. Dubillard, U. Ekström, E. Eliav, T. Enevoldsen, E. Faßhauer, T. Fleig, O. Fossgaard, L. Halbert, E. D. Hedegård, T. Helgaker, B. HelmichParis, J. Henriksson, M. van Horn, M. Iliaš, Ch. R. Jacob, S. S. Komorovský, O. Kullie, J. K. Lrdahl, C. V. Larsen, Y. S. Lee, N. H. List, H. S. Nataraj, M. K. Nayak, P. Norman, A. Nyvang, G. Olejniczak, J. Olsen, J. M. H. Olsen, A. Papadopoulos, Y. C. Park, J. K. Pedersen, M. Pernpointner, J. V. Pototschnig, R. di Remigio, M. Repisky, K. Ruud, P. Salek, B. Schimmelpfennig, B. Senjean, A. Shee, J. Sikkema, A. Sunaga, A. J. Thorvaldsen, J. Thyssen, J. van Stralen, M. L. Vidal, S. Villaume, O. Visser, T. Winther, S. Yamamoto, and X. Yuan, available at <https://doi.org/10.5281/zenodo.7670749>, see also <https://www.diracprogram.org>.
- [34] M. G. Kozlov and L. N. Labzowsky, *J. Phys. B* **28**, 1933 (1995).
- [35] K. Gaul and R. Berger, *J. Chem. Phys.* **152**, 044101 (2020).
- [36] K. Gaul and R. Berger, [arXiv:2312.08858](https://arxiv.org/abs/2312.08858).
- [37] T. Chupp and M. Ramsey-Musolf, *Phys. Rev. C* **91**, 035502 (2015).
- [38] T. E. Chupp, P. Fierlinger, M. J. Ramsey-Musolf, and J. T. Singh, *Rev. Mod. Phys.* **91**, 015001 (2019).
- [39] J. S. M. Ginges and V. V. Flambaum, *Phys. Rep.* **397**, 63 (2004).
- [40] E. A. Hinds and P. G. H. Sandars, *Phys. Rev. A* **21**, 471 (1980).
- [41] H. M. Quiney, J. K. Laerdahl, K. Fægri, and T. Saue, *Phys. Rev. A* **57**, 920 (1998).
- [42] O. P. Sushkov, V. V. Flambaum, and I. B. Khriplovich, *Zh. Eksp. Teor. Fiz.* **87**, 1521 (1984) [*Sov. Phys. JETP* **60**, 873 (1984)].
- [43] V. V. Flambaum and I. B. Khriplovich, *Phys. Lett. A* **110**, 121 (1985).
- [44] A.-M. Mårtensson-Pendrill and P. Öster, *Phys. Scr.* **36**, 444 (1987).
- [45] V. V. Flambaum and J. S. M. Ginges, *Phys. Rev. A* **65**, 032113 (2002).
- [46] N. J. Stone, *At. Data Nucl. Data Tables* **90**, 75 (2005).
- [47] P. A. M. Dirac, *Math. Proc. Cambridge Philos. Soc.* **26**, 376 (1930).
- [48] J. C. Slater, *Phys. Rev.* **81**, 385 (1951).
- [49] S. H. Vosko, L. Wilk, and M. Nuisar, *Can. J. Phys.* **58**, 1200 (1980).
- [50] K. Gaul and R. Berger, *J. Chem. Phys.* **147**, 014109 (2017).
- [51] A. D. Becke, *J. Chem. Phys.* **98**, 5648 (1993).
- [52] J. P. Perdew, K. Burke, and M. Ernzerhof, *Phys. Rev. Lett.* **77**, 3865 (1996).
- [53] C. Adamo and V. Barone, *J. Chem. Phys.* **110**, 6158 (1999).
- [54] A. D. Becke, *J. Chem. Phys.* **98**, 1372 (1993).
- [55] J. F. Stanton, J. Gauss, L. Cheng, M. E. Harding, D. A. Matthews, and P. G. Szalay, “CFOUR, Coupled-Cluster techniques for Computational Chemistry, a quantumchemical program package,” With contributions from A. Asthana, A. A. Auer, R. J. Bartlett, U. Benedikt, C. Berger, D. E. Bernholdt, S. Blaschke, Y. J. Bomble, S. Burger, O. Christiansen, D. Datta, F.

- Engel, R. Faber, J. Greiner, M. Heckert, O. Heun, M. Hilgenberg, C. Huber, T.-C. Jagau, D. Jonsson, J. Jusélius, T. Kirscher, M.-P. Kitsaras, K. Klein, G. M. Kopper, W. J. Lauderdale, F. Lipparini, J. Liu, T. Metzroth, L. A. Mück, D. P. O'Neill, T. Nottoli, J. Oswald, D. R. Price, E. Prochnow, C. Puzzarini, K. Ruud, F. Schiffmann, W. Schwalbach, C. Simmons, S. Stopkowicz, A. Tajti, J. Vázquez, F. Wang, J. D. Watts, C. Zhang, X. Zheng, and the integral packages MOLECULE (J. Almlöf and P. R. Taylor), PROPS (P. R. Taylor), ABACUS (T. Helgaker, H. J. Aa. Jensen, P. Jørgensen, and J. Olsen), and ECP routines by A. V. Mitin and C. van Wüllen. For the current version, see <http://www.cfour.de>.
- [56] D. A. Matthews, L. Cheng, M. E. Harding, F. Lipparini, S. Stopkowicz, T.-C. Jagau, P. G. Szalay, J. Gauss, and J. F. Stanton, *J. Chem. Phys.* **152**, 214108 (2020).
- [57] P.-O. Widmark, P.-Å. Malmqvist, and B. O. Roos, *Theor. Chim. Acta* **77**, 291 (1990).
- [58] V. Veryazov, P.-O. Widmark, and B. O. Roos, *Theor. Chem. Acc.* **111**, 345 (2004).
- [59] B. O. Roos, R. Lindh, P.-Å. Malmqvist, V. Veryazov, and P.-O. Widmark, *J. Phys. Chem. A* **108**, 2851 (2004).
- [60] Y. Chamorro, A. Borschevsky, E. Eliav, N. R. Hutzler, S. Hoekstra, and L. F. Pašteka, *Phys. Rev. A* **106**, 052811 (2022).
- [61] K. G. Dyall, *J. Phys. Chem. A* **113**, 12638 (2009).
- [62] K. G. Dyall, *Theor. Chem. Acc.* **135**, 128 (2016).
- [63] L. Visscher and K. G. Dyall, *At. Data Nucl. Data Tables* **67**, 207 (1997).
- [64] M. Hubert and T. Fleig, *Phys. Rev. A* **106**, 022817 (2022).
- [65] P. A. B. Haase *et al.* (NL-eEDM Collaboration), *J. Chem. Phys.* **155**, 034309 (2021).
- [66] M. Denis, Y. Hao, E. Eliav, N. R. Hutzler, M. K. Nayak, R. G. E. Timmermans, and A. Borschevsky, *J. Chem. Phys.* **152**, 084303 (2020).
- [67] K. Gaul and R. Berger, *Phys. Rev. A* **101**, 012508 (2020).
- [68] A. Zakharova, I. Kurchavov, and A. Petrov, *J. Chem. Phys.* **155**, 164301 (2021).
- [69] A. Zakharova and A. Petrov, *Phys. Rev. A* **103**, 032819 (2021).
- [70] C. Zülch, K. Gaul, S. M. Giesen, R. F. G. Ruiz, and R. Berger, [arXiv:2203.10333](https://arxiv.org/abs/2203.10333).
- [71] C. Zülch, K. Gaul, and R. Berger, *Isr. J. Chem.* **63**, e202300035 (2023).
- [72] D. Patterson and J. M. Doyle, *Phys. Rev. Lett.* **111**, 023008 (2013).
- [73] M. Verma, A. M. Jayich, and A. C. Vutha, *Phys. Rev. Lett.* **125**, 153201 (2020).
- [74] Y. Takahashi, C. Zhang, A. Jadbabaie, and N. R. Hutzler, *Phys. Rev. Lett.* **131**, 183003 (2023).
- [75] C. Zhang, P. Yu, A. Jadbabaie, and N. R. Hutzler, *Phys. Rev. Lett.* **131**, 193602 (2023).
- [76] M. Jung, *J. High Energy. Phys.* **05** (2013) 168.
- [77] T. Fleig and M. Jung, *J. High Energy. Phys.* **07** (2018) 012.
- [78] K. Gaul, S. Marquardt, T. Isaev, and R. Berger, *Phys. Rev. A* **99**, 032509 (2019).
- [79] K. Gaul, M. G. Kozlov, T. A. Isaev, and R. Berger, *Phys. Rev. Lett.* **125**, 123004 (2020).
- [80] K. Gaul, M. G. Kozlov, T. A. Isaev, and R. Berger, *Phys. Rev. A* **102**, 032816 (2020).
- [81] D. Cho, K. Sangster, and E. A. Hinds, *Phys. Rev. A* **44**, 2783 (1991).
- [82] J. de Vries, E. Mereghetti, and A. Walker-Loud, *Phys. Rev. C* **92**, 045201 (2015).
- [83] K. B. Ng, Y. Zhou, L. Cheng, N. Schlossberger, S. Y. Park, T. S. Roussy, L. Caldwell, Y. Shagam, A. J. Vigil, E. A. Cornell, and J. Ye, *Phys. Rev. A* **105**, 022823 (2022).
- [84] Y. Zhou, J. O. Island, and M. Grau, *Phys. Rev. A* **109**, 033107 (2024).
- [85] See Supplemental Material at <http://link.aps.org/supplemental/10.1103/PhysRevA.109.042819> for electronic-structure-enhancement factors of \mathcal{P} , \mathcal{T} violation for Ra-containing molecular ions shown in Table VII obtained at levels of HF and DFT employing various exchange correlation functionals. Moreover we provide additional plots showing restriction of two dimensional subspaces of the \mathcal{P} , \mathcal{T} -odd parameter space, which include the parameters d_e , $d_{sr,p}$, and k_s .